Functional Materials Letters
Vol. 10, No. 4 (2017) 1750034 (6 pages)

DOI: 10.1142/S1793604717500345

World Scientific
www.worldscientific.com

Reduced graphene oxide encapsulated Cu_2O with controlled crystallographic facets for enhanced visible-light photocatalytic degradation

Guosong Wu*, Qiuping Shen*, Houlin Yu*, Tingyu Zhao*, Congda Lu† and Aiping Liu*,‡,§
*Center for Optoelectronics Materials and Devices
Zhejiang Sci-Tech University, Hangzhou 310018, P. R. China
†Laboratory of E&M (Zhejiang University of Technology)
Ministry of Education & Zhejiang Province, Hangzhou 310014, P. R. China
‡State Key Laboratory of Nonlinear Mechanics
Institute of Mechanics, Chinese Academy of Sciences
Beijing 100190, P. R. China
§liuaiping1979@gmail.com

Received 6 February 2017; Accepted 7 April 2017; Published 26 April 2017

The Cu_2O/reduced graphene oxide (Cu_2O/rGO) composites with effective crystallographic facet controlling of Cu_2O crystals were fabricated through a simple one-step wet chemistry method. The crystallographic facet-dependent photocatalytic performance of Cu_2O was confirmed, favoring the cuboctahedral Cu_2O with {100} and {111} facets and a better photocatalytic activity when compared to cubic and octahedral ones. This was attributed to the slight difference of surface energy between {100} and {111} facets which served as a driving force to promote the separation of photogenerated electron–hole pairs. Moreover, the introduction of two-dimensional rGO sheets could accelerate the transfer of photogenerated electrons from Cu_2O to rGO, which further promoted the separation of photogenerated electron–hole pairs and the degradation of methyl orange (MO) under visible-light irradiation. The cuboctahedral Cu_2O/rGO composite exhibited a superb photocatalytic performance with the degradation percentage of MO about 97.6% after one periodic photocatalysis due to the synergistic effect of cuboctahedral Cu_2O and rGO sheets, foreboding its potential application as photocatalyst.

Keywords: Cu_2O/rGO composite; crystallographic facet control; photocatalytic activity; synergistic effect.

With the increasing problem of environmental pollution, particularly serious drinking water safety induced by organic contaminations has become the focus of attention. Photocatalytic degradation of organic dyes under visible-light irradiation through effective, cheap and stable catalysts is a good strategy.[1–4] Semiconductor-based nanocomposites with unique physical and chemical properties are regarded as ideal candidates and photocatalysts to solve the above problems. Among these, Cu_2O as an intrinsic *p*-type semiconductor (band gap of 2.2 eV) can effectively absorb and utilize solar spectrum in the visible-light region.[5,6] Additionally, low-cost and easy-to-prepare Cu_2O crystals with different exposed crystallographic facets show many controllable optical, electrical and catalytic properties, indicating their preponderance as photocatalysts.[7] However, many factors limit the photocatalytic efficiency of Cu_2O crystals including the slow electron transfer, rapid electron–hole recombination, and poor photochemical stability.[2,3,7] In order to overcome these deficiencies, many attempts have been carried out to extend the wavelength range of photoresponse, increase light-harvesting and charge-separating efficiency at the material interface, and improve the photochemical stability by constructing Cu_2O-semiconductor (Cu_2O/TiO_2[5] and Cu_2O/ZnO[8]) heterojunctions, or introducing high-conductive materials (noble metal[9] and graphene[10–12]). Until now, the research on structural, optical and photocatalytic tunability of Cu_2O-based photocatalysts is still limited and critically important since photocatalytic activity is sensitively dependent upon synergistic properties of components in composites.

In this paper, we fabricated Cu_2O/rGO (reduced graphene oxide) composites with desired crystallographic facets by a simple one-step wet chemistry approach. By changing the additional amount of structure-directing agent, we successfully adjusted the morphology, crystallographic facet orientation and optical property of Cu_2O/rGO composites. The crystallographic facet-dependent photocatalytic activities of these composites were confirmed by the degradation of methyl orange (MO) under visible-light irradiation.

§Corresponding author.

Additionally, the two-dimensional rGO sheets with good chemical stability and rapid electron transfer ability[13,14] were also verified with excellent coagents in increasing charge-separating efficiency at the Cu_2O-rGO interface and improving the efficiency of photocatalytic degradation of MO. Our result is helpful for understanding the synergistic effect of Cu_2O and rGO on the tunable optical and photocatalytic performance of composites.

GO was synthesized according to the previously reported method.[15] For Cu_2O/rGO preparation, typically, 0.173 g of $CuCl_2{\cdot}2H_2O$ and a certain amount of polyvinylpyrrolidone ($C_6H_5Na_3O_7{\cdot}2H_2O$) were dissolved into 100 mL GO aqueous solution (0.1 mg/mL). Then, 10 mL of NaOH solution (2 mol/L) was added slowly and stirred together for 30 min. After that, 10 mL of ascorbic acid (AA) solution (0.65 mol/L) was added slowly and reacted for 3 h until the precipitates were filtered and washed with D.I. water. The temperature of water bath was controlled at 55°C with vigorous magnetic stirring during entire processes. In order to investigate crystallographic facet effect on photocatalytic performance, different Cu_2O/rGO composites were prepared by changing the additional amounts of $C_6H_5Na_3O_7{\cdot}2H_2O$ (0.55 g, 3.3 g and 8.8 g), and the corresponding Cu_2O/rGO products were labeled as S_1 (cubic Cu_2O/rGO), S_2 (cuboctahedral Cu_2O/rGO) and S_3 (octahedral Cu_2O/rGO), respectively. The pure Cu_2O crystals with these three morphologies were also synthesized through a similar process except for the addition of GO solution.[16]

Morphologies and structures of the samples were observed by a Field emission scanning electron microscopy (FESEM, Hitachi S4800) and a Transmission electron microscopy (TEM, Hitachi H-7650). Crystalline structures of the samples were analyzed on a X-ray diffraction (XRD, Bruker AXS D8) with Cu K_α ($\lambda = 1.5406$ Å). X-ray photoelectron spectroscopy (XPS) was performed on a KRATOS AXIS ULTRA-DLD. Raman spectra were recorded on a Thermo Fisher DXR Raman spectrometer using a He–Ne laser ($\lambda = 632.8$ nm). Optical properties of samples were obtained through a Hitachi U-3900 UV-vis spectrophotometer and a Hitachi F7000 fluorescence spectrophotometer. Photocurrent test was conducted on a CHI 660D electrochemical work station (Shanghai Chenhua Instrument Co., China) in a three-electrode cell. The photocatalytic performances of samples were conducted by the photodegradation of MO solution under visible-light irradiation by using a 300 W xenon lamp (CEL-HXF300 Beijing Aulight Co., Ltd, China) assembled with a UV cutoff filter ($\lambda > 400$ nm) and placed 10 cm away from the suspension. During irradiation process, the suspension consisting of 50 mL MO solution (20 mg/L) and 20 mg catalyst sample was magnetically stirred and kept at room temperature by a circular water cooling system. The degradation percentage was calculated by measuring MO solution absorption at each irradiation time interval (C) and the one of the initial concentrations (C_0) at adsorption–desorption equilibrium (1 h in dark prior to irradiation). Reactive species trapping experiments were performed to investigate the reactive species involved in dye molecule degradation.

Figure 1 shows the SEM images of Cu_2O crystals and Cu_2O/rGO composites. The Cu_2O crystals with diameter about 1 μm present cubic (six exposed $\{100\}$ facets), cuboctahedral (six exposed $\{100\}$ facets and eight exposed $\{111\}$ facets) and octahedral (eight exposed $\{111\}$ facets) morphologies (Figs. 1(a)–1(c)). For Cu_2O/rGO composites, they still maintain the cubic, cuboctahedral and octahedral morphologies of Cu_2O crystals with compactly encapsulated by rGO sheets (Figs. 1(d)–1(f)). From the TEM image of cubic Cu_2O/rGO composites (S_1) (Fig. 2(a)), the Cu_2O particles are well anchored on rGO sheet surfaces. The boundary of two components in the HRTEM image (Fig. 2(b)) is clearly recognizable, and the lattice fringe spacing of 0.247 nm is corresponded to $\{111\}$ facet of Cu_2O. The element mapping obtained by energy dispersive spectroscopy in Figs. 2(c)–2(e) shows uniform distribution of Cu, O and C elements.

Figure 3 shows XPS, Raman and XRD results of Cu_2O/rGO composites. The high-resolution C 1s spectrum in Fig. 3(a) can be fitted into three peaks at 284.8 eV, 285.7 eV and 287.4 eV, assigned to C=C, C–C and C–O bonds, respectively.[14,15] The peaks at 932.6 eV and 952.6 eV are attributed to Cu $2p_{3/2}$ and Cu $2p_{1/2}$, respectively (Fig. 3(b)). The binding energy of 932.6 eV is typically associated with Cu^+ species in the Cu 2p spectrum, indicating the existence of main Cu_2O. The Raman spectra in Fig. 3(c) show two characterization ranges. A weaker peak at around 630 cm^{-1} can be ascribed to the defects caused from the symmetry destruction of Cu_2O lattice,[11] and the intensity of defect peak flows in the order of $S_2 > S_3 > S_1$. This could be related to the oxygen defect in semiconductor/rGO composite and might be affected by interfacial electronic properties of composites due to the composition difference in the semiconductor[17,18] and be helpful for the enhancement of photocatalytic performance.[19] For the rGO and GO sheets, two main peaks at around 1330 cm^{-1} and 1595 cm^{-1} belong to the characteristic signals of disordered sp^2-hybridized carbon associated with structural defects (D band) and well-order E_{2g} phonon scattering of sp^2-hybridized carbon (G band), respectively.[20] The intensity ratio of I_D/I_G increases from 0.92 for GO to 1.16 ± 0.02 for rGO, demonstrating the enhanced structure disordering and successful reduction of GO to rGO.[12,14,15] The XRD curves in Fig. 3(d) indicate the pure Cu_2O crystals of face-centered cubic phase (JCPDS card No. 05-0667),[7] whether if GO took part in the chemical reaction. No obvious distinction can be found except for the

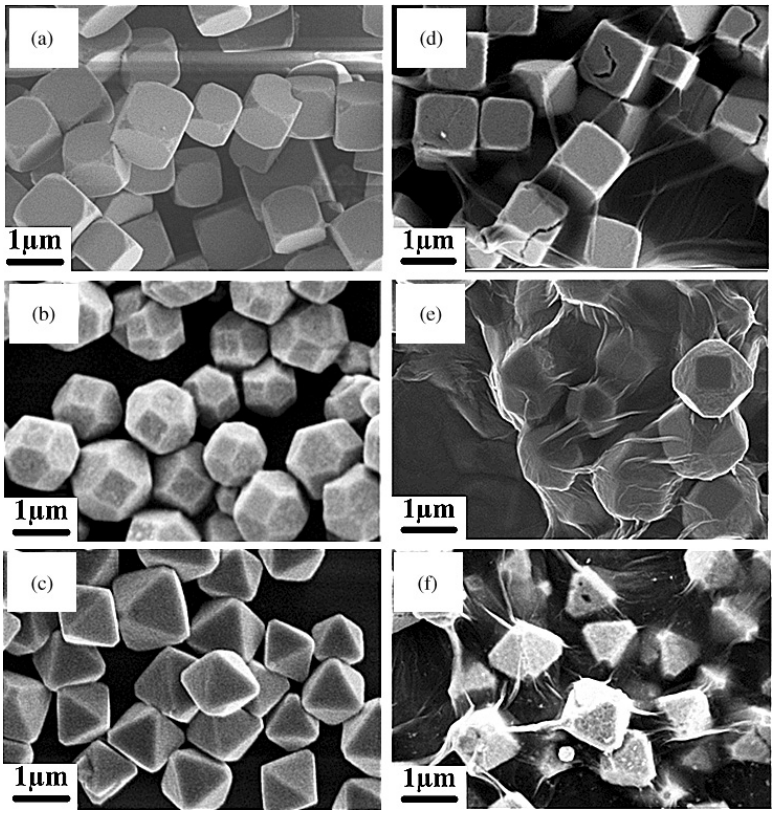

Fig. 1. SEM images of (a) cubic, (b) cuboctahedral, (c) octahedral Cu_2O, (d) cubic Cu_2O/rGO, (e) cuboctahedral Cu_2O/rGO and (f) octahedral Cu_2O/rGO.

change of peak intensity for Cu_2O crystals with different morphologies because of random particle orientations. The diffraction peak of GO sheets at $2\theta = 10.4^\circ$ disappears, indicating GO reduction to rGO and oxygen-containing functional groups removing.[15,20] Note that the diffraction peak of rGO sheets is so weak compared with Cu_2O ones that it cannot be displayed.

The influence of Cu_2O morphology on photocatalytic activity is also investigated. From Figs. 4(a)–4(f), we find that the cuboctahedral Cu_2O/rGO composite (S_2) presents

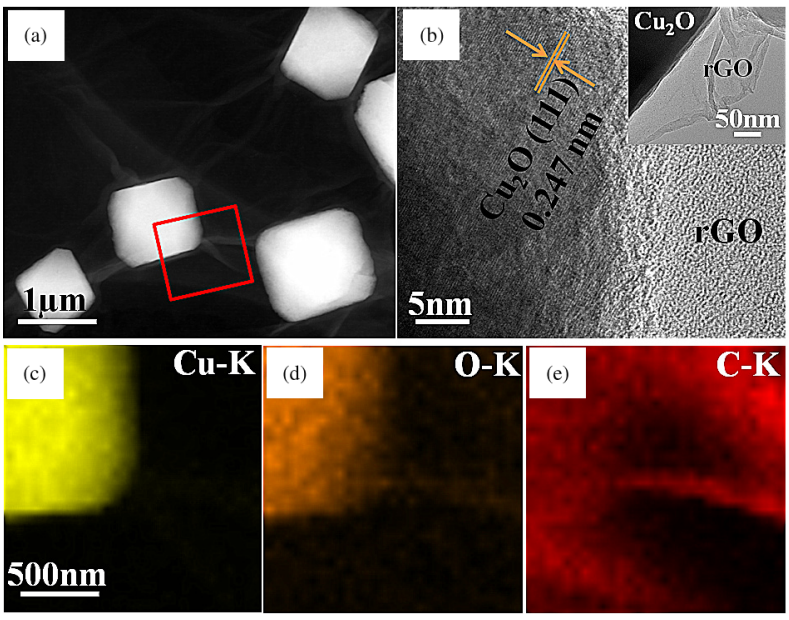

Fig. 2. (a) TEM, (b) HRTEM and (c)–(e) EDS mapping images of cubic Cu_2O/rGO composite.

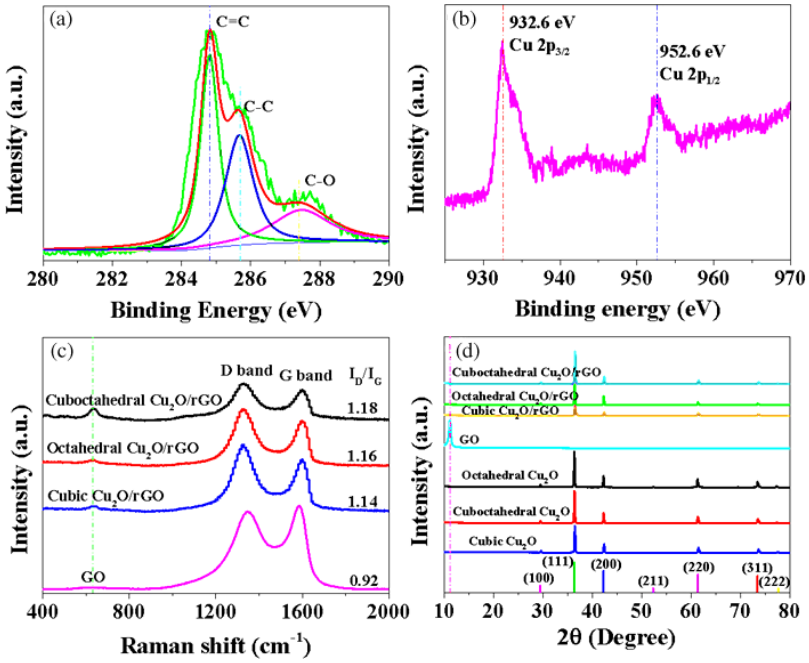

Fig. 3. XPS spectra of cuboctahedral Cu_2O/rGO composite: (a) C 1 *s*; (b) Cu 2*p*; (c) Raman spectra of different Cu_2O/rGO composites and GO; and (d) XRD spectra of different samples.

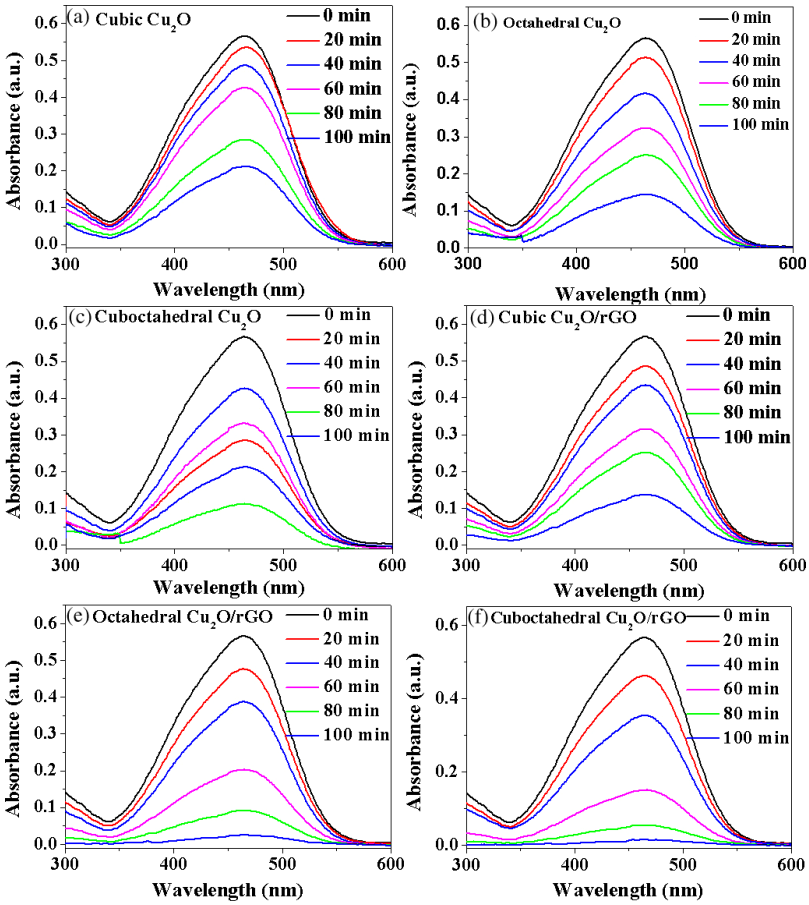

Fig. 4. Variation in the UV-vis absorbance spectra of MO solution in the presence of different photocatalysts under visible-light irradiation for 100 min: (a) cubic Cu_2O, (b) octahedral Cu_2O, (c) cuboctahedral Cu_2O, (d) cubic Cu_2O/rGO composites, (e) octahedral Cu_2O/rGO composites, and (f) cuboctahedral Cu_2O/rGO composites.

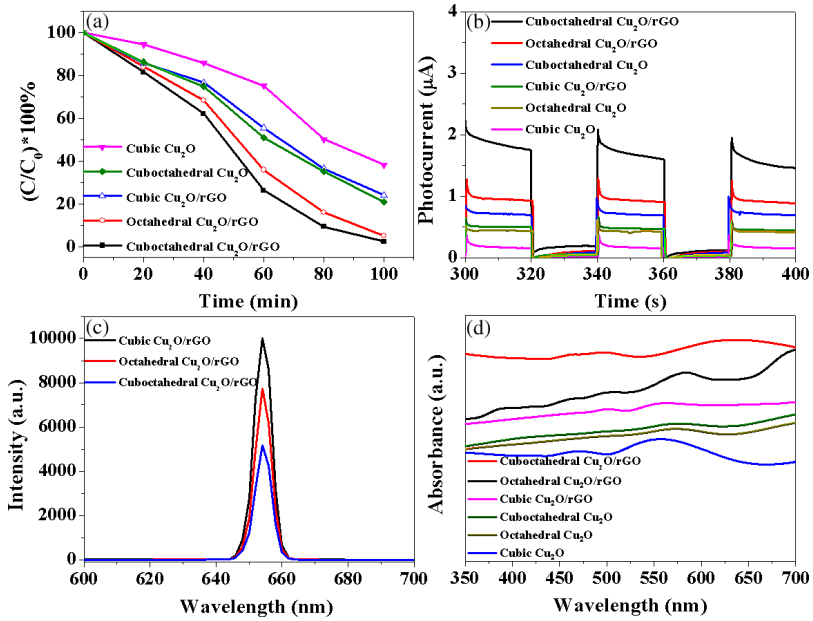

Fig. 5. (a) Photocatalytic degradation of MO as a function of irradiation time in the presence of various photocatalysts under visible-light irradiation (after adsorption–desorption equilibrium). (b) *I–T* curves, (c) PL spectra and (d) UV-vis absorbance spectra of different photocatalysts.

the rapidest degradation rate of MO after a period of 100 min under visible-light irradiation with the residual MO percentage about 2.4% (Fig. 5(a)) when compared to cubic Cu_2O (38.2%), cuboctahedral Cu_2O (21.1%), cubic Cu_2O/rGO (S_1, 23.0%) and octahedral Cu_2O/rGO (S_3, 5.1%), respectively. Such excellent photocatalytic activity of cuboctahedral Cu_2O/rGO composite could be reasoned as follows: (i) the cuboctahedral Cu_2O with exposed {100} and {111} facets promotes the separation of photogenerated electron–hole pairs by the surface energy difference between these two facets[7]; (ii) rGO improves the conductivity of composite catalysts, promoting the charge transfer process and photocatalytic efficiency. The decisive influence of crystallographic facets of Cu_2O and conductivity of rGO sheets on the photocatalytic performance of Cu_2O/rGO composite is further confirmed by photocurrent and optical behavior measurements. From the transient photocurrent (*I–T*) curves in Fig. 5(b), which are usually used as indicators for detecting the electron–hole pair recombination rate in the materials, pure cuboctahedral Cu_2O with {100} and {111} facets present a higher photocurrent than cubic Cu_2O and octahedral Cu_2O. This hints that the surface energy difference between {100} and {111} facets could serve as a driving force to promote the separation of photogenerated electron–hole pairs.[7,17,18] When rGO sheets are introduced into the system, the Cu_2O/rGO composite, especially cuboctahedra Cu_2O/rGO demonstrates the highest photocurrent, hinting its prominent photoelectric conversion effect. The photoluminescence (PL) spectra in Fig. 5(c) (another effective indicator for both the transfer process and recombination process of charge carriers) also display a similar changing tendency to the *I–T* curves. The intensity of PL peak at around 650 nm follows the order of $S_1 > S_3 > S_2$, which indicates that the fastest transfer rate and slowest recombination rate of interface charge carriers of S_2,[5,6] favoring the cuboctahedral Cu_2O/rGO composite superior photocatalytic performance than both cubic and octahedral ones. From the UV-vis absorbance spectra in Fig. 5(d), we find that pure Cu_2O crystals have a visible absorption peak at around 560–580 nm. The introduction of rGO sheets leads to an obvious red shift of absorption peak and broadening of absorbance range. One possible reason is that the synergetic effect of Cu_2O and rGO could promote the separation of photogenerated electron–hole pairs, and then leads to a slight change of bandgap structure.[5] Especially for cuboctahedral Cu_2O/rGO composite, the synergetic effect of Cu_2O and rGO is more obvious. The surface energy difference between {100} and {111} facets for cuboctahedral Cu_2O might first drive the separation of photogenerated electron–hole pairs and lead to the aggregation of holes at the {100} facets and electrons at the {111} facets.[17] Therewith, the electrons quickly transfer to conductive rGO sheets, resulting in effective separation of electron–hole pairs[11,14] and further enhancement in the photocatalytic performance of samples,[12] as shown in schematic illustration in Fig. 6(a). The photocatalytic degradation mechanism of dye molecule on the catalyst is investigated via reactive species trapping experiments by using four scavengers, namely disodium ethylenediaminetetraacetate (EDTA), isopropyl alcohol (IPA), *p*-benzoquinone (BQ) and carbon

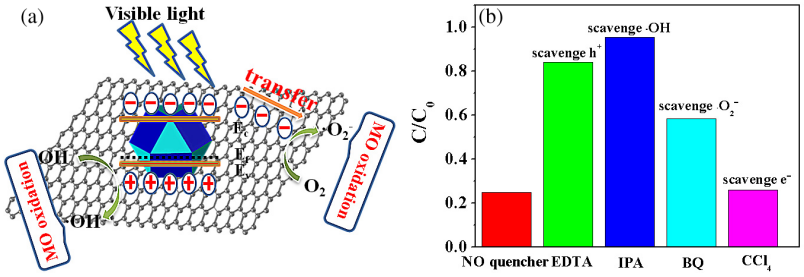

Fig. 6. (a) Schematic illustration of the generation and transfer of electron–hole pairs in the cuboctahedral Cu_2O/rGO composite under visible-light irradiation and (b) Trapping experiment of active species during the photodegradation of MO in the presence of cuboctahedral Cu_2O/rGO photocatalyst and different scavengers under visible-light irradiation.

tetrachloride (CCl_4) as holes, ·OH, $\cdot O_2^-$ and e^- scavengers, respectively. The introduction of EDTA or IPA suppresses the photocatalytic degradation of MO, indicating that the h^+ and ·OH are the main reactive species during MO degradation (Fig. 6(b)).

In summary, a facile one-step method has been developed to synthesize Cu_2O/rGO composites. The crystallographic facet controllable Cu_2O and conductive rGO play critical roles in speeding up the separation of electron–hole pairs and improving photocatalytic performance by increasing the transmission path and creating more active species. The Cu_2O/rGO composites with optimized cuboctahedral Cu_2O show excellent photocatalytic performance in the removal of MO under visible-light irradiation with the photocatalytic effect about 97.6%, indicating their potential as efficient photocatalysts for organic dye degradation.

Acknowledgments

This work was supported by the National Natural Science Foundation of China (Nos. 51572242 and 51272237), the Zhejiang Provincial Natural Science Foundation of China (Nos. LY16E020011 and LY15F050013), the Opening Fund of State Key Laboratory of Nonlinear Mechanics and the Program for Innovative Research Team of Zhejiang Sci-Tech University (No. 15010039-Y).

References

1. H. Tong *et al.*, *Adv. Mater.* **24**, 229 (2012).
2. P. Zhang *et al.*, *Acc. Chem. Res.* **49**, 911 (2016).
3. X. B. Chen *et al.*, *Chem. Rev.* **110**, 6503 (2010).
4. H. P. Wu *et al.*, *Langmuir* **33**, 407 (2017).
5. S. N. Xiao *et al.*, *Nano Lett.* **15**, 4853 (2015).
6. J. B. Cui *et al.*, *Nano Lett.* **15**, 6295 (2015).
7. W. C. Huang *et al.*, *J. Am. Chem. Soc.* **134**, 1261 (2011).
8. A. E. Kandjani *et al.*, *Langmuir* **31**, 10922 (2015).
9. B. Lu *et al.*, *Langmuir* **32**, 3085 (2016).
10. F. G. Xu *et al.*, *Electrochim. Acta* **88**, 59 (2013).
11. W. X. Zou *et al.*, *Appl. Catal., B* **181**, 495 (2016).
12. S. Z. Deng *et al.*, *J. Am. Chem. Soc.* **134**, 4905 (2012).
13. W. S. Hummers, Jr. *et al.*, *J. Am. Chem. Soc.* **80**, 1339 (1958).
14. Y. W. Zhu *et al.*, *Adv. Mater.* **22**, 3906 (2010).
15. D. C. Marcano *et al.*, *ACS Nano* **4**, 4806 (2010).
16. D. F. Zhang *et al.*, *J. Mater. Chem.* **19**, 5220 (2009).
17. L. Z. Zhang *et al.*, *Chem. Commun.* **50**, 192 (2014).
18. R. G. Li *et al.*, *Nat. Commun.* **4**, 1432 (2013).
19. X. J. Bai *et al.*, *Langmuir* **29**, 2097 (2013).
20. A. P. Liu *et al.*, *ACS Appl. Mater. Interfaces* **8**, 25210 (2016).